# Chemically and Mechanically Recyclable Vitrimers from Carbon Dioxide-Based Polycarbonates

Seiyoung Yoon,<sup>‡</sup> Satej S. Joshi,<sup>‡</sup> Sophia Aracri,<sup>‡</sup> Yuliana Ospina-Yepes, Devavrat Sathe, Mark D. Foster, \* Junpeng Wang, \* James M. Eagan\*

School of Polymer Science and Polymer Engineering, The University of Akron, Akron, Ohio 44325-3909, United States.

\*Correspondence should be addressed to mdfl@uakron.edu, jwang6@uakron.edu, or eagan@uakron.edu

<sup>‡</sup>These authors contributed equally to this work

#### **Abstract**

Designing thermoset materials with dynamic crosslinks is an important strategy to mitigate rising global carbon dioxide emission levels. The development of polymers from sustainable feedstocks, with efficient manufacturing methods, for high-value applications, and with circular end-of-use solutions is essential for advancing material technologies. One approach involves exploiting carbon dioxide itself as feedstock to create high performance, sustainable materials, by enchaining 50 mol% CO<sub>2</sub> via copolymerization with epoxides to yield polycarbonates. This work describes the synthesis, end-functionalization, and curing of poly(propylene carbonate) (PPC) and poly(cyclohexene carbonate) (PCHC) into beta-hydroxy ester vitrimers. These vitrimers

demonstrate the ability to be mechanically reprocessed up to 3 times with retention of the material's properties through dynamic transesterification exchange reactions. The polycarbonate vitrimers with gel fractions exceeding 90 % exhibit high tensile strength (> 50 MPa) and Young's modulus (> 2 GPa), achieved by varying repeat unit structure in the polymer backbone from the low  $T_g$  PPC to the more rigid high  $T_g$  PCHC structures. Owing to an entropically favorable chain back-biting mechanism, the network chains can be cleaved and depolymerized into cyclic small molecules. In the case of PCHC, this process enables repolymerization back to polycarbonates with 69 wt.%  $CO_2$  retention through life-cycles. The promising mechanical performance and recyclability of these  $CO_2$ -based polycarbonate vitrimers indicate their potential for sustainable, high-performance materials, paving the way for future innovations in circular polymer technologies and carbon capture utilization.

**Keywords**: Vitrimers, carbon dioxide polymerization, recycling, reprocessing, covalent adaptable networks (CANs).

#### Introduction

Carbon dioxide is a low cost, abundant, and sustainable co-monomer for producing polymer materials without directly impacting land-use. <sup>1-4</sup> The direct utilization of CO<sub>2</sub> by copolymerization with epoxide has developed extensively with regards to catalysis and polymer synthesis. <sup>5-8</sup> Through these advances, applications of epoxide/CO<sub>2</sub> polycarbonates as thermoplastic elastomers, films, and precursors to polyurethanes have realized commercial viability. <sup>6,9-12</sup> The synthesis of polycarbonate networks, <sup>13-17</sup> dynamic networks <sup>18,19</sup> and vitrimers from these sustainable feedstocks, however, is less studied and presents an opportunity to develop low-carbon materials as recyclable thermosets.

Dynamic networks are characterized by their ability to exchange bonds at elevated temperatures, rendering them malleable, reformable, and mechanically reprocessable.<sup>20</sup> Several dynamic crosslinking strategies based on amine, thiol, boronate, and ester moieties. <sup>21–23</sup> Of these, βhydroxyester vitrimers, derived from the reaction of epoxides and carboxylic acids, were judged particularly well-suited for introducing vitrimeric behavior into epoxide/CO<sub>2</sub> polycarbonates due to the prospect of selectively activating exchange reactions in the presence of the depolymerizable polycarbonate backbone.<sup>24,25</sup> Relevant prior work into polyester dynamic transesterification includes synthesis of polylactide networks crosslinked by urethane moieties using Sn(Oct)2 as a transesterification and curing catalyst.<sup>26</sup> Additionally, photo-induced transesterification of oligoaniline-polyester vitrimers has also been reported, using triazabicyclodecene (TBD) as the catalyst.<sup>27</sup> Hydroxyester vitrimers can also facilitate transesterification through neighboring group participation such as hydroxylated or aminated comonomers (Fig. S22).<sup>28–30</sup> This neighboring group participation approach leverages hydridic monomers, such as malic acid (MA) and citric acid, which contain β-hydroxyl groups and intramolecular H-bonds that promote the exchange reaction.<sup>31–33</sup> Recently, Rorrer and coworkers developed low-viscosity epoxy/anhydride derived polyester networks that exhibit dynamic exchange in the presence of imidazole catalysts and can be chemically recycled through stoichiometric methanolysis of the ester moieties.<sup>34</sup>

In addition to mechanical reprocessability, it may be desirable to have chemical recyclability of a network under certain end-of-use scenarios. For example, polycarbonate vitrimers from the reaction of butanediol with a highly strained bis-cyclic carbonate co-monomer can be mechanically recycled via dynamic transcarbonation exchange reactions or can be degraded under mild acidic conditions to yield the ring-opened monomer.<sup>35</sup> Recently, Detrembleur and co-workers utilized N,S exchange reactions to synthesize dissociative dynamic networks from a CO<sub>2</sub>-derived

alkylidene oxazolidone. The networks could be dissociated at 200 °C, yielding the monomers with 80% of the CO<sub>2</sub> chemically retained within the recovered structures.<sup>36</sup>

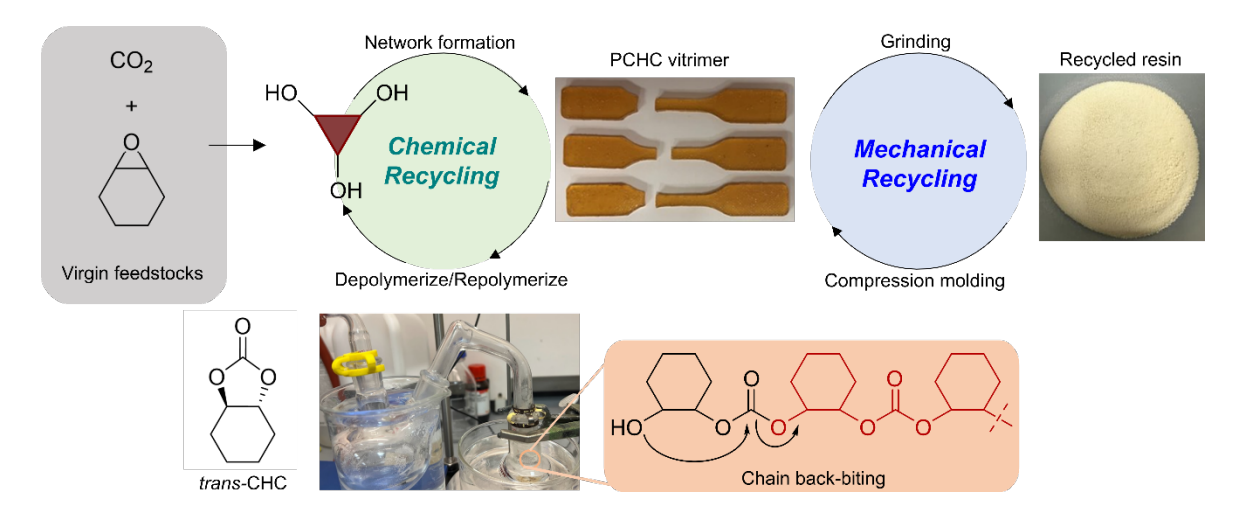


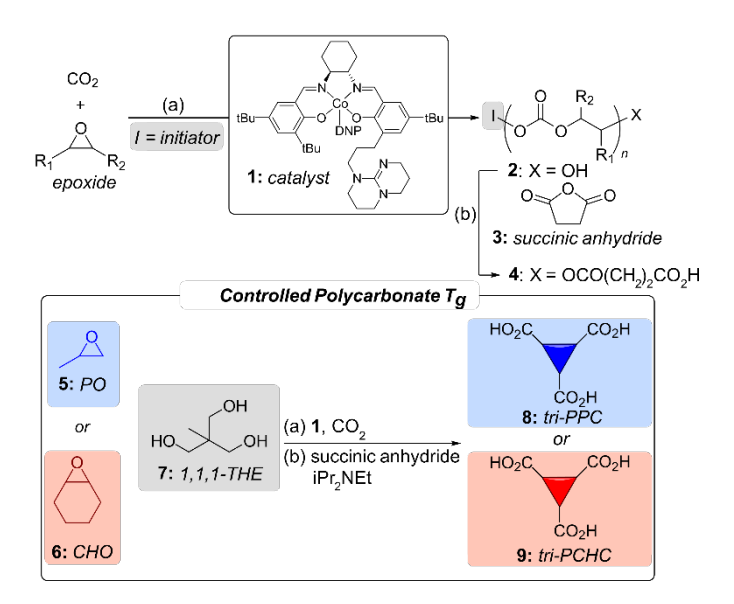
Figure. 1 Circularity of rigid CO<sub>2</sub>-based PCHC vitrimers described in this work.

Motivated by the development of sustainable thermosets, we herein report epoxide/CO<sub>2</sub>-derived polycarbonate networks crosslinked by dynamic β-hydroxy ester linkages which are both mechanically and chemically recyclable (**Figure 1**). The precursors are designed with low molecular weights (e.g., ca. 2000 g/mol) and multifunctionality to obtain optimized viscosity and aid in network formation. The networks' glass transition temperatures and mechanical properties can be controlled through selection of the epoxide comonomer. Furthermore, the curing kinetics, network relaxation properties, and end-of-use circularity are discussed. Through this comprehensive analysis, we discuss the mechanistic selectivity that enables activation of the ester crosslinks while suppressing back-biting depolymerization, thereby enhancing the material's recyclability and durability.

# Results and discussion

# Polycarbonate synthesis

Our design for epoxide/CO<sub>2</sub> polycarbonate networks focused on a synthetic approach for multifunctional (i.e., 3-armed), perfectly alternating, low-viscosity, end-functionalized polymers. To achieve this, we first synthesized hydroxyl- terminated polycarbonates using a TBD-tethered cobalt salen catalyst 1, originally discovered by Lu and coworkers, <sup>37</sup> in combination with a trifunctional initiator, 1,1,1-tris(hydroxymethyl)ethane 7 (Scheme 1). Perfectly alternating poly(propylene carbonate) (PPC) and poly(cyclohexene carbonate) (PCHC) were prepared from propylene oxide (PO) 5 and cyclohexene oxide (CHO) 6, respectively. Molar masses of 2000 g/mol were targeted for lowering the viscosity of the precursors (Fig. S7). The trifunctional initiator, 1,1,1-tris(hydroxymethyl)ethane not only facilitated the synthesis, but also served as a convenient reference in the <sup>1</sup>H NMR spectrum (s,  $\delta = 1.04-1.08$  ppm) for molecular weight and functionalization analysis (Fig. S1–S4). The experimental molar masses were determined by <sup>1</sup>H NMR to be 2250 and 1620 g/mol for PPC and PCHC, respectively. Unique to catalyst 1, the polymerization tolerates high loadings of initiator relative to catalyst (up to 1:1000) while preserving polymerization activity in the absence of solvent. Trifunctional PPC-OH and PCHC-OH were thus synthesized with relatively low catalyst loadings (0.015 mol% for PCHC and 0.006 mol% for PPC).



Scheme 1. Synthesis and chain-end functionalization of epoxide/CO<sub>2</sub> polycarbonates PPC and PCHC, (a) PPC synthesis: propylene oxide (904 mmol, 17,320 equiv.), 1,1,1-tris(hydroxymethyl)ethane (50 mmol, 480 equiv.), catalyst 1 (0.052 mmol, 1 equiv.), CO<sub>2</sub> (2.8 MPa, excess), 22 °C, 72 h; PCHC synthesis: cyclohexene oxide (794 mmol, 6352 equiv.), 1,1,1-tris(hydroxymethyl)ethane (60 mmol, 480 equiv.), catalyst 1 (0.125 mmol, 1 equiv.), CO<sub>2</sub> (2.8 MPa, excess), 22 °C, 96 h (b) polycarbonate polyol (1 equiv. to –OH end-groups), succinic anhydride (2 equiv.), iPr<sub>2</sub>NEt (0.25 equiv.), acetone.

The hydroxyl chain-ends of PPC and PCHC were then converted to carboxylic acids to form dynamic β-hydroxy ester crosslinking by reacting with commercial epoxy (DGEBA). End-capping the polyols was achieved by reacting trifunctional PPC–OH or trifunctional PCHC–OH with two equivalents of succinic anhydride (per –OH end-group) in acetone. The use of 25 mol% iPr<sub>2</sub>EtN was found to promote the complete conversion of hydroxyl chain end-groups to carboxylic acid groups. This conversion was quantified by the downfield shift of end-group methine protons in both PPC and PCHC via <sup>1</sup>H NMR (Fig. S1–S4) which was corroborated by the integration of the initiator (Fig. S2 andS4) methyl protons at 1.04–1.08 ppm. Using this method, the carboxylic acid

functionalized PPC–COOH and PCHC–COOH 3-armed precursors were synthesized on >100 g scales, as shown in Scheme 1, Fig. S8, and Tables S1 and S2. While the  $T_{\rm g}$ s of the PPC and PCHC were relatively unaffected by the end-capping procedure, we did observe a 10–15 °C increase in  $T_{\rm d}$  upon anhydride capping. The improved thermal stability of the COOH-terminated polycarbonates is attributed to the absence of the alcohol chain-ends, which can initiate the backbiting depolymerization. Thermal degradation now requires a backbone chain-scission event to begin, which requires a higher temperature.

# Vitrimer curing

As shown in Fig. 2A, the polycarbonate vitrimers were synthesized from acid-capped trifunctional polycarbonates (i.e., 8: tri-PPC and 9: tri-PCHC) and DGEBA (11), yielding catalystfree networks (13). In addition, malic acid (10: MA) was explored as a diacid spacer to manipulate the weight fraction of polycarbonate backbone and to enhance the transesterification-based bond exchange of the β-hydroxy ester through neighboring group participation to yield activated networks (12). <sup>28,29</sup> This neighboring group activation provides an alternative to traditional external catalysts commonly used in curing polymer networks involving the reaction between carboxylic acids and epoxides.<sup>31–33</sup> While Lewis acid or base catalysts are commonly used to facilitate both the curing process and dynamic bond exchange,<sup>22</sup> they pose the risk of initiating back-biting depolymerization of the polycarbonate backbone for this system. This operating window between manufacturing and depolymerization is a crucial consideration for any kinetically trapped polymer.<sup>38</sup> Therefore, precise formulation, particularly regarding the amount and choice of catalyst is imperative to prepare a vitrimer without compromising the integrity of the polycarbonate backbone during both the curing and mechanical recycling processes. Fig. 2 illustrates the curing reaction and kinetics of the PCHC vitrimers at 150 °C for different formulations. When no catalyst was used for the curing process, a network with a 98% gel-fraction, calculated using eqn. 2, was obtained after curing at 150 °C for 72 h (13). The high gel-fraction achieved, despite the prolonged heating, indicates negligible degradation into cyclic carbonates. In addition, the catalyst-free PPC vitrimer achieved a gel-fraction of over 99% after 48h of curing at 150 °C.

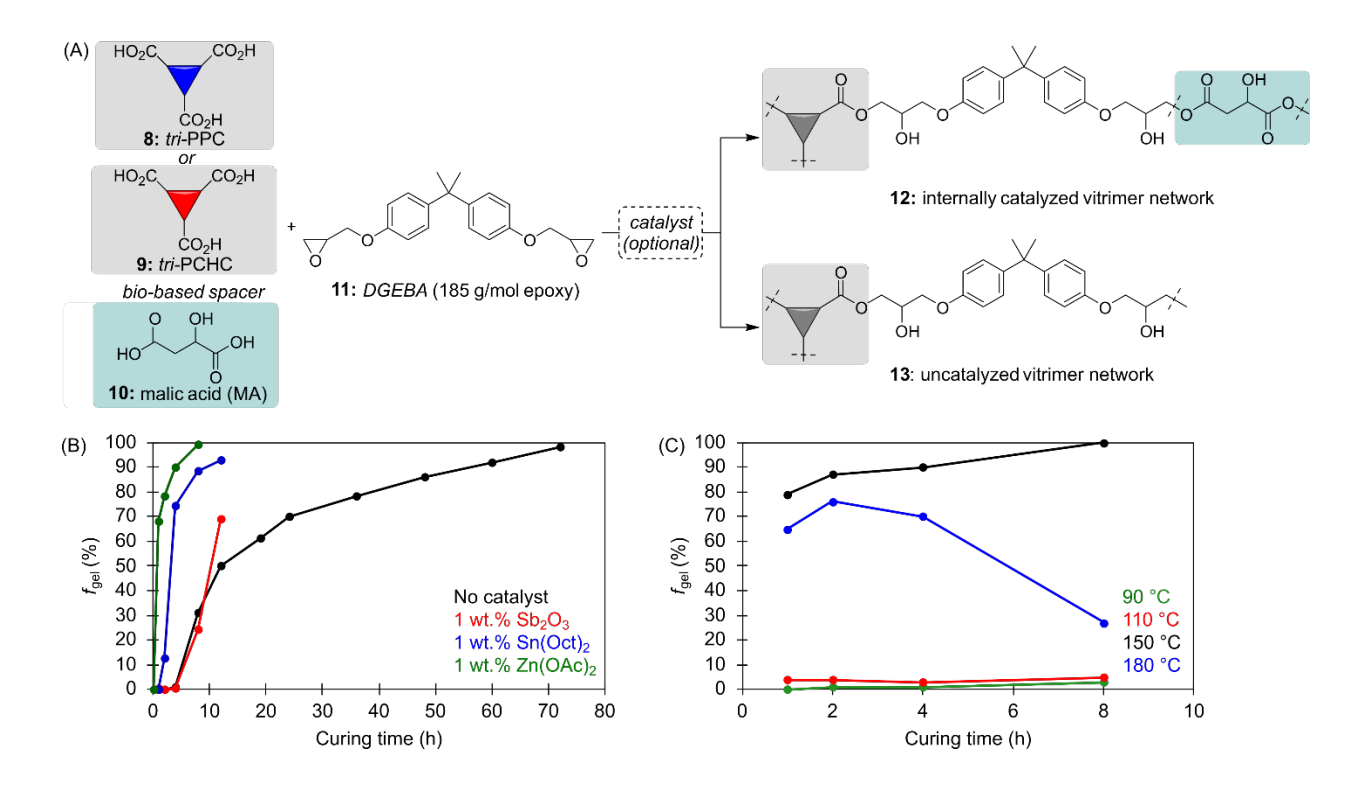


**Figure 2.** (A) Reaction scheme of curing polycarbonates with DGEBA utilizing malic acid as a bio-based diacid spacer and optional external catalyst. (B) The curing kinetics of PCHC vitrimer formulations with different catalysts at 150 °C, and (C) the curing kinetics of PCHC vitrimers with 5 mol% of zinc acetate at different temperatures.

To identify a suitable catalyst for curing the vitrimer, several Lewis acid catalysts, including Sb<sub>2</sub>O<sub>3</sub>, Sn(Oct)<sub>2</sub>, and Zn(OAc)<sub>2</sub>, were screened in the PCHC formulation, and the gel-fractions of the networks at 8 h were compared. The purpose of this experiment was to maximize gel-fraction since the introduction of soluble fraction can plasticize the polymer networks, decreasing the

mechanical properties. While facilitated curing is desirable, as this study aims to develop materials in high strength materials, it is crucial to maintain the mass fraction of polycarbonates and avoid sacrificing the thermomechanical properties. To minimize the decrease in mechanical properties from the introduction of catalysts, the mass fraction of the catalysts was kept at 1% of the final product. When introduced into the network at the same mass fraction, Zn(OAc)<sub>2</sub> led to the fastest curing of the network (Fig. 2B). This enhanced curing rate could be attributed to the stronger Lewis acidity and the higher molar equivalence of Zn(OAc)<sub>2</sub> compared to other tested catalysts. Notably, none of the catalysts led to a decrease in gel-fraction during the curing process, at 1 wt.% and 150 °C indicating that the extent of back-biting degradation of trifunctional PCHC-COOH was negligible. Isothermal TGA analysis during the curing process with higher loadings such as 5 mol% Zn(OAc)<sub>2</sub> (Fig. S25) shows negligible degradation of the vitrimer resin at 150 °C over the entire curing process, further supporting the absence of the back-biting degradation. However, when all catalyst concentrations were maintained at 5 mol.%, a decrease in gel fraction was observed for the Sn(Oct)2 catalyst, suggesting catalyst-induced back-biting degradation in this formulation (Fig. S24). Meanwhile, the vitrimer with 5 mol.% Sb<sub>2</sub>O<sub>3</sub> exhibited slower curing than the vitrimer with 5 mol.% Zn(OAc)<sub>2</sub>, further confirming that Zn(OAc)<sub>2</sub> serves as the optimal catalyst for this system. Lewis bases such as tertiary amines resulted in lowering the onset of depolymerization and competing crosslinking/back-biting reactions. Although the PCHC networks could be obtained with high gel-fractions, some challenges in their manufacture should be noted. Due to the high  $T_{\rm g}$ of the PCHC precursors, the precursors must be mixed at elevated temperature. However, the rapid curing of the network at 150 °C results in a rapid increase in viscosity, impeding efficient mixing. Fig. 2C illustrates that only a minor increase in gel-fraction was observed when the mixture was heated at 90 °C or 110 °C for 8 h. This insignificant increase in gel-fraction at elevated temperature

provides a practical window for mixing and degassing the materials before curing at 150 °C. However, curing the mixture at 180 °C resulted in a decrease in gel-fraction, which could be attributed to the competing crosslinking reaction and the back-biting degradation. Therefore, 180 °C is the upper limit of the cure temperature for these formulations.

An increase in  $T_g$  was seen for both tri-PPC-COOH ( $T_g = 12$  °C) and tri-PCHC-COOH ( $T_g = 12$  °C) 61 °C) after crosslinking them into vitrimers ( $T_{\rm g} \sim 45$  and 90 °C, respectively). This effect can be attributed to limited chain mobility due to formation of crosslinks with the bulky aromatic groups of the DGEBA crosslinker (Fig. S11 and S12). All PCHC-based formulations had similar  $T_{\rm g}$ s (86– 91°C), regardless of the presence of malic acid, suggesting the polycarbonate dominates the segmental motion in the network. However, dynamic mechanical thermal analysis (DMTA) of the malic acid containing network (Fig. S26) did reveal a lower crosslinking density and Tg of 85 °C, which was 5 °C lower than the measurement by DSC. A similar increase was observed for  $T_d$ , with both PPC and PCHC materials showing a 20 °C increase after crosslinking (Fig. S10). The higher  $T_{\rm d}$ s can be explained by the presence of crosslinks, which impede the ability of the free hydroxyl groups to initiate back-biting depolymerization of the carbonate backbone. Additionally, as discussed in the description of the carboxylic acid precursors above, the end-capping of trifunctional PPC-OH and PCHC-OH, contributes to enhanced thermal stability. In the vitrimer formulation with Zn(OAc)<sub>2</sub>, the T<sub>d</sub> decreased by 5 °C to 265 °C. This decrease is likely due to the presence of Zn(OAc)<sub>2</sub>, which can promote the chain-scission of the polycarbonate backbone.

**Table 1.** Tensile properties for PCHC and PPC vitrimers measured by uniaxial tensile testing.

Entry (#)	Polycarbonate (1 equiv) <sup>a</sup>	DGEBA (equiv)	MA (equiv)	Zn(OAc) <sub>2</sub> (equiv.)	fgel <sup>b</sup> (%)	$T_g^c$ (°C)	σbreak (MPa)	Ebreak (%)	E <sup>d</sup> (GPa)	
1	PCHC	1.5	-	-	95	91	$35 \pm 4$	1.9 ±	2.30 ±	
								0.3	0.50	

2	PCHC	1.5	-	0.15	93	86	$34 \pm 5$	2.9 ±	_	$\pm$
								0.8	0.08	
3	PCHC	3.0	1.5	-	94	90 <sup>e</sup>	40 ± 1	3.5 ±		±
								0.1	0.07	
4	PCHC	3.0	1.5	0.3	98	87	$32 \pm 15$	4.1 ±		±
								1.4	0.26	
5	PPC	3.0	1.5	-	93	46	58 ± 7	7.2 ±	0.70	±
								0.8	0.07	

<sup>a</sup>equiv. defined by the mmol of COOH end-group for the trifunctional polymers. <sup>b</sup>determined by sol-gel study in acetone, <sup>c</sup>reported for  $2^{nd}$  heating run by differential scanning calorimetry (heating/cooling rate = 10 °C/min), <sup>d</sup>reported for initial slope by uniaxial tensile testing (deformation rate = 5 mm/min), <sup>e</sup>DMTA data showing  $T_g$  of 85 °C and lower crosslink density is provided in supporting information (Fig. S26)

#### Vitrimer mechanical properties

Mechanical properties of the virgin vitrimer formulations, evaluated using uniaxial tensile tests, are shown in Fig. 3, Fig. S13, and Table 1. The PPC/DGEBA/MA formulation resulted in the highest tensile strength,  $58 \pm 7$  MPa, and highest percent elongation at break,  $7.2 \pm 0.8\%$ . However, it also resulted in the lowest Young's modulus,  $0.93 \pm 0.07$  GPa. The PCHC/DGEBA and PCHC/DGEBA/MA formulations produced tensile strengths ( $35 \pm 4$  and  $40 \pm 1$  MPa, respectively), but the formulation without MA yielded a larger Young's modulus and smaller percent elongation at break, making it comparatively more brittle. We propose that the increase in elongation at break with the addition of MA could be due to the increase of molecular weight between crosslinks that comes with incorporation of MA into the network (Fig. S26). It is difficult to identify a general trend for the impact of  $Zn(OAc)_2$  on the mechanical properties' average values. In the PCHC formulation with MA, the addition of  $Zn(OAc)_2$  seems to increase the uncertainty in the value of tensile strength, but not for the formulation without MA. The samples made with MA and  $Zn(OAc)_2$  had more visible surface defects, which likely contribute to the larger scatter in the tensile strength value. Given the importance of thermosets in high-modulus

and high- $T_{\rm g}$  composite applications, we elected to focus on the PCHC system, despite PPC's higher toughness at room temperature.

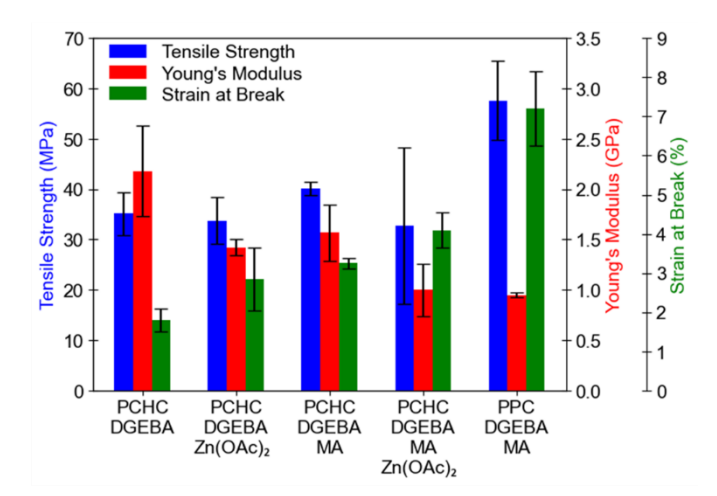


**Figure 3.** Tensile properties of virgin samples with various formulations. Detailed values shown in Table 1.

# Mechanical reprocessing of vitrimers

It is necessary to avoid chemical degradation of the PCHC backbone of the vitrimer during the mechanical reprocessing to maintain the mechanical properties. Isothermal TGA was conducted to check the mass integrity at elevated temperatures and decide what temperature to use for reprocessing to avoid thermal decomposition caused by the back-biting degradation of PCHC. Slight weight reductions of 1.1% and 1.8% were observed over 2 h at 160 °C and 170 °C, respectively (Fig. S14). Since the mechanical reprocessing requires heat-pressing of the ground materials for a prolonged time to allow exchange reactions and network relaxations to take place, the reprocessing experiments were conducted at 160 °C to provide a balance of good mobility for healing and minimization of the PCHC backbone degradation. To achieve smaller ground vitrimer particles without compromising the integrity of the PCHC backbone, ball milling was conducted at -196 °C by circulating liquid nitrogen over the outer surface of the ball milling jar during the

milling process. After ball milling at -196 °C for 10 min, a fine powdered vitrimer was obtained (Fig. 4). To assess the effectiveness of mechanical reprocessing, reprocessing was carried out for one, two, or three cycles before testing the properties of the reprocessed samples. Heat-pressing of the finely ground vitrimer at 160 °C and 13.8 MPa resulted in reprocessed samples that had smooth surfaces and enhanced mechanical properties. The  $T_{\rm g}$ s of the reprocessed vitrimer samples were consistently above 80 °C (Fig. S15). Additionally, the gel-fraction of the vitrimer samples remained above 90% independent of the number of reprocessing cycles. These results indicate the effective suppression of mechanochemical degradation of the PCHC backbone during reprocessing. Interestingly, both the  $T_{\rm g}$  and the gel-fraction of the vitrimer samples increased slightly with reprocessing. These increases can be attributed to post-curing (Fig. S16) and more uniform dispersion of the Zn(OAc)<sub>2</sub> catalyst during the ball milling process.

Comparison of tensile mechanical properties of the reprocessed samples with those of the virgin samples in Fig. 4 provides evidence that the vitrimers can be effectively reprocessed at least twice, without a decrease in the mechanical properties (Table S3). The tensile strength, strain at break, and Young's modulus for the virgin samples were  $33 \pm 15$  MPa,  $1.8 \pm 0.3$  GPa,  $2.1\% \pm 0.2\%$ , respectively. With the first reprocessing, the average tensile strength increased by 30% and the average strain at break by 75%. The average properties after the second reprocessing were comparable to those after the first. However, the tensile strength and strain at break values decreased by ca. 5% and the Young's modulus value by 30% with the third cycle of reprocessing.

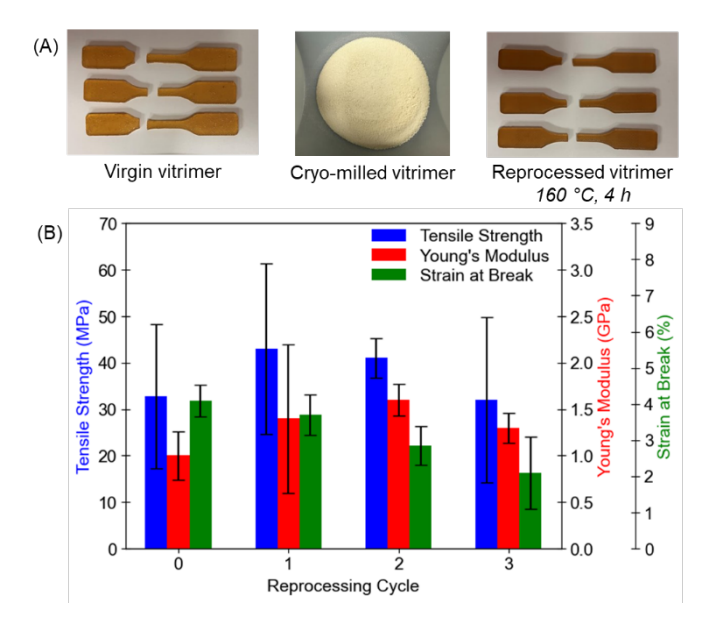


**Fig. 4** Mechanical recycling of PCHC vitrimers (entry 4, Table 1) by cryo-milling followed by heat-pressing at 160 °C. (A) Photos of samples before reprocessing, during, and after. (B) Tensile properties of virgin and reprocessed samples.

Measurements of storage modulus as a function of temperature (Fig. 5) combined with density measurements (Table S4) provide valuable insights into how crosslinking density evolves with reprocessing. Consistent with the variation of tensile strength with reprocessing, the crosslinking density, calculated using eqn. 1, increased markedly with the first reprocessing cycle and remained above that of the virgin material for the second and third reprocessing, though dropping somewhat from the value for the sample reprocessed only once. There are two possible reasons for the significant improvement in the mechanical properties with the first reprocessing. First, the cryogenic ball milling used to break down the vitrimer before remolding appears to improve the dispersion of the Zn(OAc)<sub>2</sub> in the vitrimer. Zn(OAc)<sub>2</sub> does not mix readily with the other components, and the virgin samples showed lateral inhomogeneities in color. These inhomogeneities are associated with small patches of high Zn(OAc)<sub>2</sub> concentration, which

possibly led to defects (Fig. S21). In contrast, samples reprocessed from ball-milled material were optically laterally uniform, suggesting a network with fewer defects. As more zinc acetate becomes chemically dispersed within the network, each Zn metal center coordinates with two ester and carbonate groups, releasing acetic acid, which evaporates during curing and reprocessing (Fig. S23). This explanation fits well with our observation that the crosslink density from the temperature sweep measurements (Table S4) is notably higher for the once reprocessed sample than for the virgin sample, indicating the formation of additional ionic crosslinks. The cause for the crosslinking density increase after reprocessing is still under investigation, but it is clear that the PCHC/DGEBA/MA/Zn(OAc)<sub>2</sub> vitrimer network (entry 4, Table 1) exhibited excellent mechanical properties after both the first and second reprocessing. Vitrimer networks synthesized without the addition of MA were unable to be mechanically reprocessed. This observation may be attributed to the effectiveness of MA as neighboring group in accelerating the transesterification bond exchange reactions (BERs) since it can facilitate the BERs via an extra β-hydroxyl group through neighboring group participation.<sup>33</sup>

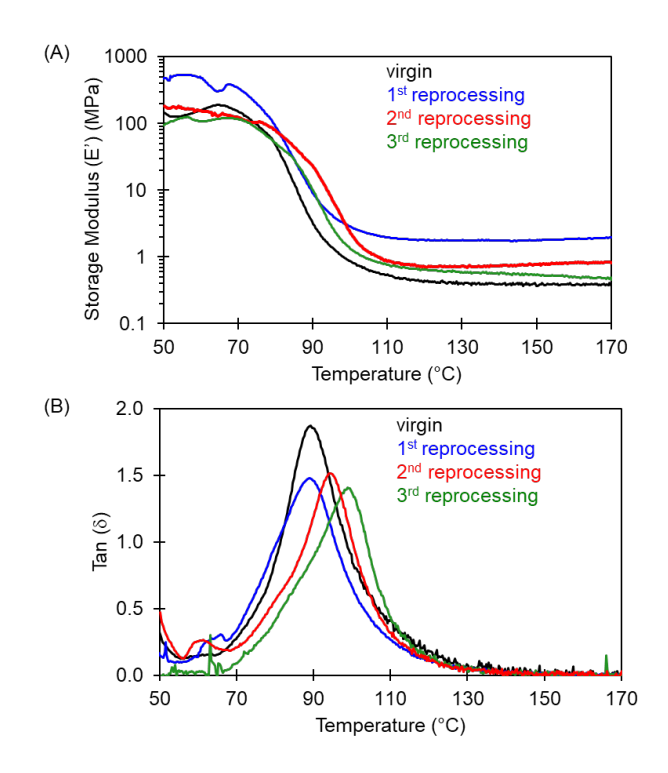


**Figure 5.** (A, B) Dynamic mechanical analysis temperature sweep results for virgin and reprocessed samples (tension mode, 0.1% strain, 1 Hz, in the TA RSA-G2 DMTA).

# Vitrimer $T_{\rm v}$ determination

The topology freezing transition temperature ( $T_v$ ) is a key parameter for understanding how these vitrimers might be mechanically recycled or reused. Two common techniques used for the determination of  $T_v$  are stress relaxation analysis<sup>26,39,40</sup> and non-isothermal creep measurement.<sup>41–43</sup> When an estimate of  $T_v$  was inferred from stress relaxation measurements,  $T_v$  was defined as the temperature at which the vitrimer attains a viscosity of  $10^{12}$  Pa·s. The stress relaxation data were fit to a stretched exponential functional form to extract a nominal macroscopic stress relaxation time,  $\tau$ , and stretching exponent,  $\alpha$ . (Fig, S17). Assuming a Maxwell model for the relationship between viscosity and shear modulus, with the storage moduli measured here, a value was calculated for  $\tau$  corresponding to a viscosity of  $10^{12}$  Pa·s. Using an Arrhenius plot of  $\tau$  vs. T (Fig.

S18) and extrapolating to the appropriate value of  $\tau$  yielded an estimate of  $T_v$  (Table S6) and the Arrhenius activation energy,  $E_a$  of the BERs (Table S5). For the sample PCHC/DGEBA/MA/Zn(OAc)<sub>2</sub> the estimate for  $T_v$  from the stress relaxation data was 165 °C (Table S6).

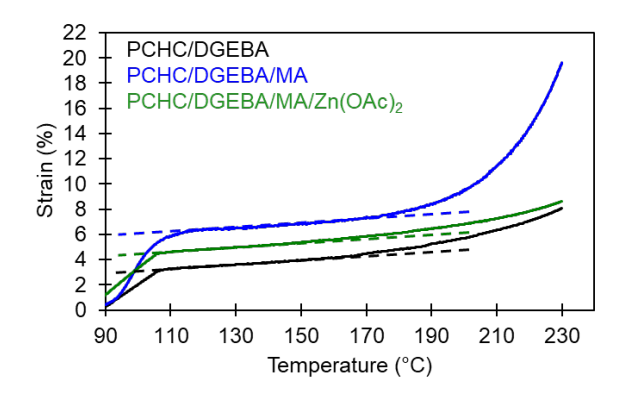


**Figure 6.** Results for non-isothermal creep measurements of virgin samples of PCHC vitrimers (tension mode in the TA RSA-G2 DMTA).

While the above method was optimal for certain ideal vitrimer systems, some uncertainties in the present polycarbonate networks complicated the determination of their  $T_v$  values. For example, the experimental stress relaxation curves reflect a shape dictated by both the vitrimeric BERs and various polymer chain relaxations and microphases. He accurse of these uncertainties, the use of non-isothermal creep measurements for determination of  $T_v$  was also explored (Fig. 6), since the flow we associate with  $T_v$  can be measured directly on experimental time scales with creep measurements. The essential premise behind the approach is that when the vitrimer temperature is ramped to  $T > T_g$ , the strain appearing in the sample due to creep varied linearly with temperature until BERs start to occur on experimental timescales. Once the BERs occurred frequently enough, the variation in strain with temperature was nonlinear. Two conventions for assigning the value of  $T_v$  using non-isothermal creep data that are seen in the literature are in some respects analogous to

the conventions by which  $T_g$  can be determined. One convention is to assign  $T_v$  to the temperature at which the deviation from initial linear behavior begins.<sup>23,39,45,46</sup> The second convention is to draw on a strain vs. T plot a line tangent to the linear behavior below  $T_{\rm v}$  and another line tangent to a region of linear behavior above  $T_v$ , with  $T_v$  assigned at the intersection of these two tangent lines. 41 For all the formulations considered here, it proved difficult to assign the tangent line above  $T_{\rm v}$  in a manner that did not seem arbitrary, so we reported values based on the onset of nonlinear creep behavior. Rather than focusing just on specific values for  $T_{\rm v}$ , it was also instructive to consider the general features of the creep curves from virgin samples shown in Fig. 6. The slopes of the construction lines tangent to the linear portions of the three curves are the same. So, at this level of analysis the creep behavior was unaffected by the incorporation of MA or by the inclusion of Zn(OAc)<sub>2</sub> for T < 165 °C. All three curves began to deviate from the linear behavior near 170  $^{\circ}$ C, indicating that the  $T_{\rm v}$  associated with onset was the same for these three formulations. This estimate of  $T_v = 170$  °C agreed well with the estimate of 165 °C from the extrapolation of stress relaxation data for PCHC/DGEBA/MA Zn(OAc)<sub>2</sub> noted before. Above 170 °C the creep behaviors of the three formulations were distinct. The formulation including the diacid spacer, PCHC/DGEBA/MA, showed a creep strain that increases with temperature much more rapidly than that of the corresponding formulation without MA. The fact that the curves for both deviated near 170 °C, but that the deviation for PCHC/DGEBA/MA was much more dramatic, was consistent with the contention that BERs are present to some extent in PCHC/DGEBA, but the kind of facile reformability sought with a vitrimer was clearly substantially enhanced when MA was included. While this enhancement aligns with expectations, the presence of BERs in PCHC/DGEBA is unexpected, as the absence of neighboring group participation and external catalysts should result in a network without BERs. Previous reports suggest that an abundance of hydroxyl groups, which serve as nucleophilic reactants, can facilitate the formation of catalyst-free hydroxy ester vitrimer materials.  $^{47,48}$  We speculate that the BERs in PCHC/DGEBA may arise from the abundance of esters and carbonates along the polycarbonate backbone, which act as electrophilic reactants and the catalysis from the trace amount of residual tethered cobalt salen catalyst and iPr<sub>2</sub>EtN in PCHC. Surprisingly, with the addition of Zn(OAc)<sub>2</sub> to PCHC/DGEBA/MA the creep was suppressed, so much so that PCHC/DGEBA/MA/Zn(OAc)<sub>2</sub> creeped less than either of the other two formulations for all T > 170 °C. So, while inclusion of Zn(OAc)<sub>2</sub> sped up the curing of the network, it possibly impeded the topological rearrangement of the network by BERs in the virgin sample due to the poor dispersion of the Zn(OAc)<sub>2</sub>

# **Chemical recycling**

The perfectly alternating addition of epoxides and CO<sub>2</sub> into the polycarbonate backbone chain affords both the maximum incorporation of CO<sub>2</sub> as well as a handle to catalytically depolymerize to entropically favored small molecules. While PPC depolymerization to cyclic propylene carbonate is well-known, only recently has PCHC depolymerization to monomer cyclohexene oxide been reported. Buchard, Lu, and Williams reported catalyst systems capable of decarbonating PCHC with high selectivity, up to 98%. <sup>49–52</sup> In these studies, acetylated end-capped polymer chains did not exhibit depolymerization due to the absence of the hydroxyl group at the chain end, which is essential for the back-biting mechanism. This complicates application to the dynamically crosslinked systems that contain succinic acid capped chain-ends.

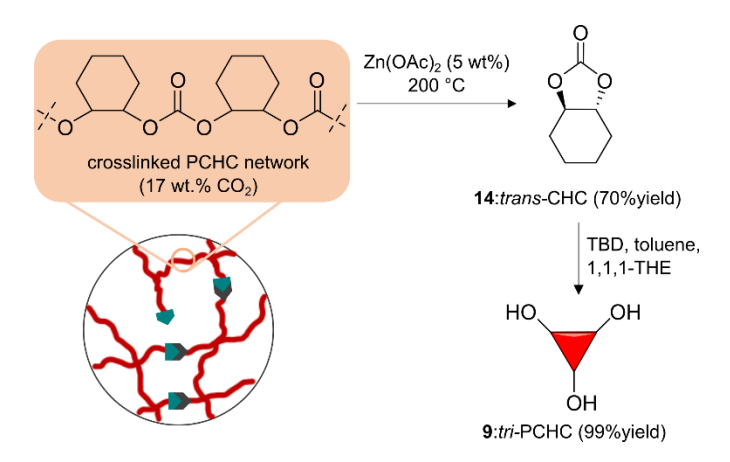


**Figure 7.** Chemical recycling of PCHC vitrimers via back-biting depolymerization followed by repolymerization to trifunctional PCHC (experimental details in Fig. S19 and S20).

All attempts with Lewis acids and nucleophilic bases to depolymerize PCHC networks resulted in the formation of trans-cyclohexene carbonate (14: trans-CHC). Specifically, the use of an additional 5 wt.% Zn(OAc)<sub>2</sub> at 200 °C under vacuum yielded pure trans-CHC in a 70% yield (Fig. S19) through a mid-chain scission initiated depolymerization. Although not the starting epoxide comonomer, the cyclic carbonate retains the CO<sub>2</sub> atom efficiency and might be suitable for repolymerization with multifunctional ring-opening polymerization. We were intrigued by a report from Guillaume and co-workers using metallic and organocatalysts such as TBD, to repolymerize trans-CHC into PCHC using benzyl alcohol as an initiator.<sup>53</sup> Using this approach, we investigated the ability to resynthesize trifunctional polycarbonates without loss of the CO<sub>2</sub> molecules (Fig. S19, S20). We observed that trans-CHC could be repolymerized using trifunctional initiator 1,1,1tris(hydroxymethyl)ethane (THE) in toluene with TBD as the ring-opening polymerization catalyst to afford  $M_{\rm n}$ s in the range of 1710–2200 g/mol (by <sup>1</sup>H NMR) with  $T_{\rm g}$ s in the range of 58–60 °C (Fig. S20), in good agreement with characteristics of the virgin PCHC. No polyether linkages from a decarboxylative ring-opening propagation mechanism were detected in the <sup>1</sup>H NMR, although some TBD-initiated species were observed (Fig. S6 and Fig. S9). This may ultimately limit the number of chemical life cycles, but still provides an improved circular life-cycle for end-capped polycarbonates. The chemical recycling experiments (Fig. 7) describe a CO<sub>2</sub>-retentive loop with 69 wt.% of the CO<sub>2</sub> incorporated as polycarbonate between life-cycles of the end-capped vitrimer networks.

#### **Conclusions**

Through this work, CO<sub>2</sub>-derived polycarbonate vitrimers that showcase excellent mechanical performance and high glass transition temperatures as well as mechanical reprocessability and chemical recyclability have been developed. Low molecular weight polycarbonate precursors were synthesized using high initiator to catalyst ratios and high productivities, owing to the use of the tethered cobalt salen system. This offers efficient scale-up routes for producing large quantities of the polycarbonate precursors from epoxides and CO<sub>2</sub>. The curing of these dynamic networks with malic acid and Zn(OAc)<sub>2</sub> accelerates the cure-time and the bond exchange behavior, and the latter contribute to the mechanical reprocessing of these materials. Using ballmilling and compression molding, the vitrimers can be reprocessed up to three times Depending on the use of PPC or PCHC as polymer backbone, a range of mechanical and thermal properties were attained owing to the contrasting glass transition temperatures and repeat unit rigidity. PPC vitrimers showed high mechanical strength (tensile strength > 50 MPa) due to higher degree of ductility compared to the more rigid PCHC vitrimers (Young's modulus > 2 GPa). These properties present an opportunity for these materials to be used in vitrimer-fiber composites according to the desired use-case.<sup>54</sup> PCHC vitrimers were also successfully mechanically recycled up to 3 cycles wherein the glass transition temperature, crosslink density and mechanical strength were improved through the first two cycles when compared to the virgin

networks. Additionally, the ability of the carbonate backbone to undergo depolymerization to cyclic *trans*-CHC and be subsequently repolymerized into *tri*-PCHC preserves the sequestered CO<sub>2</sub> (69 wt.%) in the chemicals. This approach maintains atom economy for chemical recycling, which is a green chemistry cornerstone. This work describes the potential of CO<sub>2</sub>-based polycarbonate platforms for high performance applications as effective substitutes for traditional thermosets with the distinction of circularity and carbon dioxide valorization.

#### **Experimental Section**

#### **Materials**

For polycarbonate syntheses and chain-end functionalization: Carbon dioxide (99.990 vol%) was purchased from Airgas and was used as received. Cyclohexene oxide (>98%) and propylene oxide (Reagent Plus, 99%) were purchased from Sigma-Aldrich and were dried over CaH<sub>2</sub> for 48 hours, purified via vacuum transfer and stored under N<sub>2</sub> prior to use. 1,5,7-triazabicyclo [4.4.0] dec-5-ene (TBD) tethered cobalt salen polymerization catalyst was synthesized as per reference 1. 1,1,1-tris(hydroxymethyl)ethane (1,1,1-THE) (98%) was procured from Sigma-Aldrich and was purified by dissolving in hot THF followed by precipitation in hexanes, vacuum filtration and drying under vacuum. Succinic anhydride (97%) and N,N-diisopropylethylamine (Reagent Plus, 99%) were also acquired from Sigma-Aldrich and used as received. Acidic methanol was prepared by addition of HCl (1L, 1M) to methanol (400 mL).

For COOH concentration determined by titration: Potassium hydroxide (reagent grade, >90%), potassium acid phthalate (analytical grade, >99.99%), isopropyl alcohol (reagent grade, >99.00%) and tetrahydrofuran (reagent grade, >99.00%), were purchased from Sigma-Aldrich

Chemical Company and use as received. Phenolphthalein (>98%, reagent grade) was acquired from Fisher Chemical and used as received.

For vitrimer curing: DGEBA (185 g/epoxy) was acquired from Hexion and used as received. Malic acid (99+%), zinc acetate dihydrate (98+%) were purchased from Acros Organics and were each ground to a fine powder using a mortar and pestle prior to use.

For vitrimer depolymerization: Zinc acetate dihydrate (98+%) was purchased from Acros Organics and was ground to a fine powder using a mortar and pestle prior to use. TBD tethered cobalt salen catalyst was prepared as previously reported.<sup>37</sup> (*R*,*R*)-N,N'-Bis(3,5-di-tert-butylsalicylidene)-1,2-cyclohexanediaminochromium(III) chloride, (*R*,*S*)-N,N'-Bis(3,5-di-tert-butylsalicylidene)-1,2-cyclohexanediaminochromium(III) chloride and bis(triphenylphosphoranylidene)ammonium chloride (PPNCl) (97%) were purchased from Sigma-Aldrich and were used as received and stored under nitrogen in a glovebox.

For repolymerization: TBD acquired from MilliporeSigma was stored in a nitrogen environment and used as received. Toluene (anhydrous, 99.8%) was purchased from Sigma-Aldrich and acetic acid (glacial, 99.7%) was purchased from Fisher Chemical and was used as 1.6 M solution in toluene.ds

#### Methods

Synthesis of hydroxyl terminated trifunctional poly(cyclohexene carbonate) (PCHC–OH)  $M_{\rm n,target} = 2000$  g/mol, target yield = 120 g

In a 300 mL stainless-steel pressure reactor, cobalt salen catalyst **1** (**Scheme 1**) (0.12 g, 0.125 mmol, 1 equiv.) and 1,1,1-tris(hydroxymethyl)ethane (7.21 g, 60 mmol, 480 equiv.) were

charged. Cyclohexene oxide (80.4 mL, 794 mmol, 6352 equiv.) was then added via syringe and the reactor was sealed using a Viton O-ring. The reactor was then purged with  $N_2$  for 5 minutes to remove air. The reactor was then pressurized with  $CO_2$  (2.8 MPa, excess) and polymerization was stirred for 96 h at 22 °C. At the end of the 96 h, the reaction was quenched using  $H_3PO_4$  quench solution in acetone (12 mL, 0.1 M). The polymer was dissolved in acetone (200 mL) and then precipitated in acidic methanol (500 mL, as prepared). The acetone-acidic methanol layer was decanted and the precipitated polymer was extracted in acetone, dried over MgSO<sub>4</sub>, filtered and dried under reduced pressure to afford hydroxyl terminated poly(cyclohexene carbonate) (PCHC–OH) (91 g, NMR  $M_0$  = 1620 g/mol).

Synthesis of hydroxyl terminated trifunctional poly(propylene carbonate) (PPC-OH)  $M_{\rm n,target} = 2000$  g/mol, target yield = 100 g

In a 300 mL stainless-steel pressure reactor, cobalt salen catalyst **1** (Scheme 1) (0.05 g, 0.052 mmol, 1 equiv.) and 1,1,1-tris(hydroxymethyl)ethane (5.2 g, 50 mmol, 480 equiv.) were charged. Propylene oxide (63.3 mL, 904 mmol, 17320 equiv.) was then added via syringe and the reactor was sealed using a Viton O-ring. The reactor was then pressurized with  $CO_2$  (2.8 MPa, excess) and the polymerization was stirred for 72 h at 22 °C. At the end of the 72 h, the reaction was quenched using  $H_3PO_4$  quench solution in acetone (5 mL, 0.1 M). The polymer was dissolved in acetone (200 mL) and then precipitated in acidic methanol (500 mL, as prepared). The acetone-acidic methanol layer was decanted and the precipitated polymer was extracted in acetone, dried over MgSO<sub>4</sub>, filtered and dried under reduced pressure to afford hydroxyl terminated poly(propylene carbonate) (PPC–OH) (86 g, NMR  $M_n$  = 2250 g/mol).

Synthesis of carboxylic acid terminated trifunctional poly(cyclohexene carbonate) (PCHC–COOH) 9 (Scheme 1)

In a 1 L round bottom flask, PCHC–OH (90.5 g, 167.6 mmol end-groups by NMR, 1 equiv.) was dissolved in acetone (90.5 mL). To this, succinic anhydride (33.6 g, 335.3 mmol, 2 equiv.) was added with stirring. Diisopropylethylamine (7.3 mL, 41.9 mmol, 0.25 equiv.) was then added using a syringe. The reaction mixture was stirred for 8 hours at 50 °C, under air. At the end of the 8 hours, the reaction mixture was cooled to room temperature and was precipitated in acidic methanol (500 mL, as prepared). The acidic methanol-acetone layer was decanted, the precipitated polymer was dissolved in acetone, dried over MgSO<sub>4</sub>, filtered and dried under reduced pressure to afford carboxylic acid terminated PCHC–COOH **9 (Scheme 1)** (105 g, 88 % yield, >99% end-capped,  $M_{n,NMR} = 2070$  g/mol).

Synthesis of carboxylic acid terminated trifunctional poly(propylene carbonate) (PPC–COOH) 8 (Scheme 1)

In a 1 L round bottom flask, PPC–OH (86.1 g, 140.3 mmol end-groups, 1 equiv.) was dissolved in acetone (86 mL). To this, succinic anhydride (28.1 g, 280.6 mmol, 2 equiv.) was added with stirring. Diisopropylethylamine (6.1 mL, 35.1 mmol, 0.25 equiv.) was then added using a syringe. This reaction mixture was stirred for 8 hours at 22 °C, under air. At the end of the 8 hours, the reaction mixture was precipitated in acidic methanol (500 mL, as prepared). The acidic methanol-acetone layer was decanted, the precipitated polymer was dissolved in acetone, dried over MgSO<sub>4</sub>, filtered and dried under reduced pressure to afford carboxylic acid terminated PPC–COOH **8 (Scheme 1)** (94 g, 84 % yield, >99% end-capped,  $M_{n,NMR}$  = 2380 g/mol).

PCHC/DGEBA vitrimer curing (entry 1, Table 1)

PCHC–COOH **9 (Scheme 1)** (2.9 g, 4.2 mmol end-groups) and DGEBA (0.8 g, 4.2 mmol epoxy groups) were mixed with a spatula into a paste and degassed under vacuum at 130 °C until all visible bubbles escaped from the samples (1 h). The mixture was transferred into a PTFE mold and cured at 150 °C for 72 h ( $f_{gel} = 95$  %).

# PCHC/DGEBA/Zn(OAc)2 vitrimer curing (entry 2, Table 1)

PCHC–COOH **9** (Scheme 1) (4.7 g, 6.9 mmol end-groups), DGEBA (1.3 g, 6.9 mmol epoxy groups), and zinc acetate (76 mg, 0.34 mmol, 5 mol% of PCHC end groups) were mixed with a spatula into a paste and degassed under vacuum at 110 °C until all visible bubbles escaped from the samples (2 h). It is then added into a stainless-steel mold and cured by heat pressing at 150 °C, 13.8 MPa for 8 h ( $f_{gel}$  = 93 %).

#### PCHC/DGEBA/MA vitrimer curing (entry 3, Table 1)

PCHC–COOH **9** (Scheme 1) (2.3 g, 3.4 mmol end-groups), malic acid (0.2 g, 3.4 mmol carboxylic acid groups), and DGEBA (1.3 g, 6.8 mmol epoxy groups) were mixed into a paste with a spatula and degassed under vacuum at 130 °C until all visible bubbles escaped from the samples (1 h). The mixture was then added into a PTFE mold cured at 150 °C for 72 h ( $f_{gel} = 99$ %).

# PCHC/DGEBA/MA/Zn(OAc)<sub>2</sub> vitrimer curing (entry 4, Table 1)

PCHC–COOH **9** (Scheme 1) (5.3 g, 7.7 mmol end-groups), malic acid (0.5 g, 7.7 mmol carboxylic acid groups), DGEBA (3.0 g, 15.3 mmol epoxy groups) and zinc acetate (140 mg, 0.77 mmol, 5 mol% of PCHC end groups) were mixed into a paste with a spatula and degassed under vacuum at 110 °C until all visible bubbles escaped from the samples (30 min). The

mixture was then added into a stainless-steel mold and cured by heat pressing at 150 °C, 13.8 MPa for 8 h ( $f_{gel} = 97$  %).

# PPC/DGEBA/MA vitrimer curing (entry 5, Table 1)

PPC–COOH **8 (Scheme 1)** (2.3 g, 3.4 mmol end-groups), malic acid (0.2 g, 3.4 mmol carboxylic acid groups), and DGEBA (1.3 g, 6.8 mmol epoxy groups) were mixed into a paste with a spatula and degassed under vacuum at 55 °C for 1 h. The mixture was then added into a stainless-steel mold and cured by heat pressing at 150 °C, 13.8 MPa for 24 h. The resulting sample was post-cured in an oven at 150 °C for another 24 h. ( $f_{gel} > 99$  %).

# Mechanical reprocessing of PCHC/DGEBA/MA/Zn(OAc)2 vitrimer (entry 4, Table 1)

PCHC vitrimer (5 g) was added to 50 mL stainless-steel jar along with stainless-steel balls (6 balls, d = 1.2 mm). The jar was sealed and inserted into a Retsch CryoMill and shaken at 5 Hz for 10 min while cooling with liquid nitrogen. The cooled jar was then shaken at 30 Hz for 10 min while cooling with liquid nitrogen to give fine powders of ground vitrimer. Ground vitrimer was then added to a stainless-steel mold and cured by heat pressing at 160 °C for 4 h ( $f_{gel} = 89$  %). The above procedure was repeated to make samples reprocessed for up to 3 cycles ( $f_{gel,1st}$  reprocessing = 93 %,  $f_{gel,2nd}$  reprocessing = 91 %,  $f_{gel,3rd}$  reprocessing = 91 %).

# Depolymerization of PCHC/DGEBA/MA/Zn(OAc)<sub>2</sub> vitrimer (entry 2, Fig. S19)

PCHC/DGEBA/MA/Zn(OAc)<sub>2</sub> vitrimer (entry 4, Table 1, 1 g, contains 45 wt. % PCHC units) was cryo-milled into a fine powder and added into a 15 mL round bottom flask (boiling flask). TBD tethered cobalt salen catalyst **1 (Scheme 1)** (10 mg, 1 weight % of vitrimer) was then added into the boiling flask which was then connected to a vacuum transfer bridge. A two-necked flask

(receiving flask) was connected to the vacuum transfer bridge. After setting up static vacuum, the boiling flask was heated to 200 °C and stirred for 1 h. At the end of 1 h, this system was opened to vacuum (200 mTorr) and the trans-cyclohexene carbonate (trans-CHC) was observed condensing inside the vacuum transfer bridge and receiving flask. The boiling flask was cooled to 22 °C after 24 h and trans-CHC **14** (**Fig. 7**) (0.32 g, 72% yield of carbonate moiety) was recovered and analyzed by <sup>1</sup>H NMR (Fig. S5).

# Repolymerization of trans-CHC using trifunctional initiator (entry 3, Fig. S20)

In a 1 mL vial, 1,1,1-THE (7) (6 mg, 0.05 mmol) was combined with TBD (13.9 mg, 0.1 mmol). Trans-CHC **14** (Fig. 7) (93 mg, 0.66 mmol) was added to the reaction mixture and toluene was added as solvent to make a 4 M solution with respect to trans-CHC. The reaction mixture was then stirred for 24 h at 60 °C. At the end of 24 h, the reaction mixture was cooled to room temperature and acetic acid solution (62.5 mL, 1.6 M solution in toluene) was added as quench via micropipette. The reaction mixture was concentrated by evaporating the liquids under reduced pressure followed by acetone (5 mL) extraction and precipitation in acidic methanol (10 mL, as prepared). The acidic methanol-acetone was then decanted and the precipitated polymer was dissolved in acetone and dried under reduced pressure to afford trifunctional hydroxyl terminated PCHC–OH **22** (99 mg,  $M_{n,NMR}$  = 2230 g/mol).

#### Characterization

Molecular weights ( $M_{n,GPC}$  and  $M_{w,GPC}$ ) and dispersity D ( $M_{w,GPC}/M_{n,GPC}$ ) were measured by gel permeation chromatography (GPC) in THF (2.5 mg/mL) using a Tosoh EcoSEC HLC-8320 GPC with RI detector. Molar mass calibration was set up using polystyrene standards with narrow dispersity (D = 1.05) and a flow rate of 1 mL/min.

Thermogravimetric analyses (TGA) were performed on TA Discovery TGA 550 instrument using a ramp rate of 10 °C/min under a nitrogen atmosphere. Temperatures of degradation ( $T_{\rm dS}$ ) were reported as the T where 5% weight loss was reached.

Glass transition temperatures ( $T_{\rm g}$ s) were determined using a TA Discovery DSC250 instrument. Sample runs were performed under a nitrogen atmosphere using a heat-cool-heat profile. The heating/cooling rate was 10 °C/min and  $T_{\rm g}$ s were reported for the second heating curve.

Uniaxial tensile testing was conducted at room temperature (23 °C) on an Instron 5567 instrument using ASTM D638 standard procedure with a deformation rate of 5 mm/min.

Dogbone samples of dimensions according to type V from ASTM D638 (distance between grips = 25.4 mm) were used. All values were measured in triplicate and reported as an average of three runs. The Young's moduli were reported as the slope of the initial linear part of the stress strain curve.

Dynamic mechanical thermal analysis (DMTA) tests were conducted on a TA-RSA G2 DMTA instrument in tensile mode. Samples were shaped as rectangles of dimensions 10 mm (L) X 3 mm (W) X 2 mm (T) and tested at a frequency of 1 Hz and 0.1% strain. Samples were heated from 50 to 200 °C at a ramp rate of 2 °C/min. Glass transition temperatures were reported at maximum values of  $\tan \delta$ . All measurements were made in the linear viscoelastic region. Molecular weight between cross-links ( $M_x$ ) and cross-linking density ( $u_e$ ) were calculated using the equation

where E' is the rubbery plateau modulus,  $v_e$  is the molar cross-linking density, r is the mass density measured using a density kit XPR/X SR-Ana attachment to a weighing balance, R (8.314)

J mol<sup>-1</sup> K<sup>-1</sup>) is the universal gas constant, T is the absolute temperature at the rubbery plateau and  $M_x$  is the molecular weight between cross-links.

Non-isothermal creep experiments were conducted on a TA-RSA G2 DMTA instrument in tension geometry. Rectangular samples with dimensions 60 mm (L) x 6 mm (W) x 1.5 mm (T) were prepared. The temperature was set to 80 °C, and the sample was given 15 minutes to thermally equilibrate. The experiment was started using an axial force of 0.2 N  $\pm$  0.1 N and the temperature ramped at a rate of 2 °C/min from 70 °C to 250 °C. The topology freezing transition temperature ( $T_v$ ) was identified as the temperature at which the increase in strain with temperature above the glass transition temperature became nonlinear.

Sol-gel studies were conducted by swelling a cured vitrimer sample in acetone (1 mg/mL) at 22 °C for 24 hours and determining its weight after swelling ( $w_0$ ). At the end of the 24 hours, the acetone soluble fraction was decanted, and the acetone insoluble gel was dried in a vacuum oven at 100 °C for 24 hours to ensure complete solvent removal and the weight of the dried sample ( $w_1$ ) determined. Gel fraction ( $f_{gel}$ ) was calculated as

$$f_{gel} = \frac{w_1}{w_0} \times 100\%,$$
 .....(Equation 2)

All measurements were done in triplicate and an average  $f_{\rm gel}$  value was reported.

#### ASSOCIATED CONTENT

**Supporting Information**. Detailed experimental procedures and characterization data (NMR, TGA, DSC, GPC, DMA, tensile, and stress relaxation) are available in the supporting

#### **AUTHOR INFORMATION**

# **Corresponding Author**

information document.

\*Correspondence should be addressed to <a href="mailto:mdfl@uakron.edu">mdfl@uakron.edu</a>, <a href="mailto:jwang6@uakron.edu">jwang6@uakron.edu</a>, or <a href="mailto:eagan@uakron.edu">eagan@uakron.edu</a>

#### **Author Contributions**

The manuscript was written through contributions of all authors. All authors have given approval to the final version of the manuscript. ‡These authors contributed equally.

Conceptualization – MDF, JW, JME
Data curation – SSJ, SY, SA, YOY
Formal analysis – SSJ, SY, SA, YOY, DS
Funding acquisition – MDF, JW, JME
Investigation – SSJ, SY, SA, YOY, DS
Methodology - All authors
Project administration – MDF, JW, JME
Supervision – MDF, JW, JME
Validation – SSJ, SY, SA, MDF, JW, JME
Visualization – SSJ, SY, SA, MDF, JW, JME
Writing – SSJ, SY, SA, MDF, JW, JME

# **Funding Sources**

This research was funded by the U.S. Department of Energy (USDOE), Office of Energy Efficiency and Renewable Energy (EERE), Advanced Materials and Manufacturing Technologies Office (AMMTO) and Bioenergy Technologies Office (BETO) under Bio-

Optimized Technologies for keeping Thermoplastics from the Landfill and Environment (BOTTLE) project DE-FOA-0002245-1683 (Award No. DE-EE0009297).

#### **Notes**

SSJ, SY, SA, MDF, JW, JME are inventors on a patent application of the subject materials and JME owns equity in Eterno LLC., commercializing CO<sub>2</sub>-based thermosets.

#### **ACKNOWLEDGMENT**

We wish to thank The Ohio Board of Regents, Kresge Foundation, and The National Science Foundation (CHE-0341701 and DMR-0414599) for funds used to purchase the NMR instrument used in this work.

#### **REFERENCES**

- (1) Bachmann, M.; Zibunas, C.; Hartmann, J.; Tulus, V.; Suh, S.; Guillén-Gosálbez, G.; Bardow, A. Towards Circular Plastics within Planetary Boundaries. *Nat. Sustain.* **2023**, *6*, 599–610. https://doi.org/10.1038/s41893-022-01054-9.
- (2) Grignard, B.; Gennen, S.; Jérôme, C.; Kleij, A. W.; Detrembleur, C. Advances in the Use of CO<sub>2</sub> as a Renewable Feedstock for the Synthesis of Polymers. *Chem. Soc. Rev.* **2019**, *48*, 4466–4514. https://doi.org/10.1039/C9CS00047J.
- (3) Assen, N. von der; Bardow, A. Life Cycle Assessment of Polyols for Polyurethane Production Using CO<sub>2</sub> as Feedstock: Insights from an Industrial Case Study. *Green Chem* **2014**, *16*, 3272–3280. https://doi.org/10.1039/C4GC00513A.
- (4) Assen, N. von der; Jung, J.; Bardow, A. Life-Cycle Assessment of Carbon Dioxide Capture and Utilization: Avoiding the Pitfalls. *Energy Environ. Sci.* **2013**, *6*, 2721. https://doi.org/10.1039/c3ee41151f.

- (5) Joshi, S. S.; Eagan, J. M. Homogeneous CO<sub>2</sub> Copolymerization and Coupling. In Chemical Valorisation of Carbon Dioxide; Stefanidis, G., Stankiewicz, A., Eds.; The Royal Society of Chemistry, 2022, pp 128–149. https://doi.org/10.1039/9781839167645.
- (6) Cao, H.; Wang, X. Carbon Dioxide Copolymers: Emerging Sustainable Materials for Versatile Applications. *SusMat* **2021**, *1*, 88–104. https://doi.org/10.1002/sus2.2.
- (7) Luinstra, G. Poly(Propylene Carbonate), Old Copolymers of Propylene Oxide and Carbon Dioxide with New Interests: Catalysis and Material Properties. *Polym. Rev.* **2008**, *48*, 192–219. https://doi.org/10.1080/15583720701834240.
- (8) Yang, G.; Xie, R.; Zhang, Y.; Xu, C.; Wu, G. Evolution of Copolymers of Epoxides and CO<sub>2</sub>: Catalysts, Monomers, Architectures, and Applications. *Chem. Rev.*, **2024**, *124*, 12305–12380; https://doi.org/10.1021/acs.chemrev.4c00517.
- (9) Schwarz, D. B.; Eagan, J. M. Plastics from Carbon Dioxide: Synthesis, Properties, and End-of-Life Considerations for Epoxide Copolymers; 2022; pp 469–506. https://doi.org/10.1021/bk-2022-1412.ch010.
- (10) Orgilés-Calpena, E.; Arán-Aís, F.; Torró-Palau, A. M.; Montiel-Parreño, E.; Orgilés-Barceló, C. Synthesis of Polyurethanes from CO<sub>2</sub>-Based Polyols: A Challenge for Sustainable Adhesives. *Int. J. Adhes.* **2016**, *67*, 63–68. https://doi.org/10.1016/j.ijadhadh.2015.12.027.
- (11) Alagi, P.; Ghorpade, R.; Choi, Y. J.; Patil, U.; Kim, I.; Baik, J. H.; Hong, S. C. Carbon Dioxide-Based Polyols as Sustainable Feedstock of Thermoplastic Polyurethane for Corrosion-Resistant Metal Coating. *ACS Sustain. Chem. Eng.* **2017**, *5*, 3871–3881. https://doi.org/10.1021/acssuschemeng.6b03046.

- (12) DeBolt, M.; Kiziltas, A.; Mielewski, D.; Waddington, S.; Nagridge, M. J. Flexible Polyurethane Foams Formulated with Polyols Derived from Waste Carbon Dioxide. *J. Appl. Polym. Sci.* **2016**, *133*. https://doi.org/10.1002/app.44086.
- (13) Subhani, M. A.; Köhler, B.; Gürtler, C.; Leitner, W.; Müller, T. E. Transparent Films from CO<sub>2</sub>-Based Polyunsaturated Poly(Ether Carbonate)s: A Novel Synthesis Strategy and Fast Curing. *Angew. Chem. Int. Ed.* **2016**, *55*, 5591–5596. https://doi.org/10.1002/anie.201509249.
- (14) Gao, L.; Feng, J. A One-Step Strategy for Thermally and Mechanically Reinforced Pseudo-Interpenetrating Poly(Propylene Carbonate) Networks by Terpolymerization of CO<sub>2</sub>, Propylene Oxide and Pyromellitic Dianhydride. *J. Mater. Chem. A* **2013**, *I*, 3556. https://doi.org/10.1039/c3ta01177a.
- (15) Gao, L.; Huang, M.; Wu, Q.; Wan, X.; Chen, X.; Wei, X.; Yang, W.; Deng, R.; Wang, L.; Feng, J. Enhanced Poly(Propylene Carbonate) with Thermoplastic Networks: A Cross-Linking Role of Maleic Anhydride Oligomer in CO<sub>2</sub>/PO Copolymerization. *Polymers* **2019**, *11*, 1467. https://doi.org/10.3390/polym11091467.
- (16) Huang, M.; Gao, L.; Feng, J.; Huang, X.; Li, Z.; Huang, Z.; Wang, L. Cross-Linked Networks in Poly(Propylene Carbonate) by Incorporating (Maleic Anhydride/ *Cis* -1,2,3,6-Tetrahydrophthalic Anhydride) Oligomer in CO<sub>2</sub>/Propylene Oxide Copolymerization: Improving and Tailoring Thermal, Mechanical, and Dimensional Properties. *ACS Omega* **2020**, *5*, 17808–17817. https://doi.org/10.1021/acsomega.0c02608.
- (17) Gao, L.; Chen, X.; Liang, X.; Guo, X.; Huang, X.; Chen, C.; Wan, X.; Deng, R.; Wu, Q.; Wang, L.; Feng, J. A Novel One-Pot Synthesis of Poly(Propylene Carbonate) Containing Cross-Linked Networks by Copolymerization of Carbon Dioxide, Propylene Oxide, Maleic Anhydride, and Furfuryl Glycidyl Ether. *Polymers* **2019**, *11*, 881. https://doi.org/10.3390/polym11050881.

- (18) Poon, K. C.; Gregory, G. L.; Sulley, G. S.; Vidal, F.; Williams, C. K. Toughening CO<sub>2</sub>-Derived Copolymer Elastomers Through Ionomer Networking. *Adv. Mater.* **2023**, *35*, 2302825. https://doi.org/10.1002/adma.202302825.
- (19) Gregory, G. L.; Sulley, G. S.; Kimpel, J.; Łagodzińska, M.; Häfele, L.; Carrodeguas, L. P.; Williams, C. K. Block Poly(Carbonate-ester) Ionomers as High-Performance and Recyclable Thermoplastic Elastomers. *Angew. Chem. Int. Ed.* **2022**, *61*, e202210748. https://doi.org/10.1002/anie.202210748.
- (20) Zee, N. J. V.; Nicolaÿ, R. Vitrimer Chemistry and Applications. In *Macromolecular Engineering: From Precise Synthesis to Macroscopic Materials and Applications*, ed. K. Matyjaszewski, Y. Gnanou, N. Hadjichristidis and M. Muthukumar. Wiley, 2022; pp 1–38. https://doi.org/10.1002/9783527815562.mme0029.
- (21) Scott, T. F.; Schneider, A. D.; Cook, W. D.; Bowman, C. N. Photoinduced Plasticity in Cross-Linked Polymers. *Science* **2005**, *308*, 1615–1617. https://doi.org/10.1126/science.1110505.
- (22) Montarnal, D.; Capelot, M.; Tournilhac, F.; Leibler, L. Silica-Like Malleable Materials from Permanent Organic Networks. *Science* **2011**, *334*, 965–968. https://doi.org/10.1126/science.1212648.
- (23) Van Zee, N. J.; Nicolaÿ, R. Vitrimers: Permanently Crosslinked Polymers with Dynamic Network Topology. *Prog. Polym. Sci.* **2020**, *104*, 101233. https://doi.org/10.1016/j.progpolymsci.2020.101233.
- (24) Phillips, O.; Schwartz, J. M.; Kohl, P. A. Thermal Decomposition of Poly(Propylene Carbonate): End-Capping, Additives, and Solvent Effects. *Polym. Degrad. Stab.* **2016**, *125*, 129–139. https://doi.org/10.1016/j.polymdegradstab.2016.01.004.

- (25) Darensbourg, D. J.; Yeung, A. D. Thermodynamics of the Carbon Dioxide–Epoxide Copolymerization and Kinetics of the Metal-Free Degradation: A Computational Study. *Macromolecules* **2013**, *46*, 83–95. https://doi.org/10.1021/ma3021823.
- (26) Brutman, J. P.; Delgado, P. A.; Hillmyer, M. A. Polylactide Vitrimers. *ACS Macro Lett.* **2014**, *3*, 607–610. https://doi.org/10.1021/mz500269w.
- (27) Chen, Q.; Yu, X.; Pei, Z.; Yang, Y.; Wei, Y.; Ji, Y. Multi-Stimuli Responsive and Multi-Functional Oligoaniline-Modified Vitrimers. *Chem. Sci.* **2017**, *8*, 724–733. https://doi.org/10.1039/C6SC02855A.
- (28) Liu, T.; Zhang, S.; Hao, C.; Verdi, C.; Liu, W.; Liu, H.; Zhang, J. Glycerol Induced Catalyst-Free Curing of Epoxy and Vitrimer Preparation. *Macromol. Rapid Commun.* **2019**, *40*, 1800889. https://doi.org/10.1002/marc.201800889.
- (29) Giebler, M.; Sperling, C.; Kaiser, S.; Duretek, I.; Schlögl, S. Epoxy-Anhydride Vitrimers from Aminoglycidyl Resins with High Glass Transition Temperature and Efficient Stress Relaxation. *Polymers* **2020**, *12*, 1148. https://doi.org/10.3390/polym12051148.
- (30) He, C.; Shi, S.; Wang, D.; Helms, B. A.; Russell, T. P. Poly(Oxime–Ester) Vitrimers with Catalyst-Free Bond Exchange. *J. Am. Chem. Soc.* **2019**, *141*, 13753–13757. https://doi.org/10.1021/jacs.9b06668.
- (31) Wang, S.; Teng, N.; Dai, J.; Liu, J.; Cao, L.; Zhao, W.; Liu, X. Taking Advantages of Intramolecular Hydrogen Bonding to Prepare Mechanically Robust and Catalyst-Free Vitrimer. *Polymer* **2020**, *210*, 123004. https://doi.org/10.1016/j.polymer.2020.123004.
- (32) Mu, S.; Zhang, Y.; Zhou, J.; Wang, B.; Wang, Z. Recyclable and Mechanically Robust Palm Oil-Derived Epoxy Resins with Reconfigurable Shape-Memory Properties. *ACS Sustain*. *Chem. Eng.* **2020**, *8*, 5296–5304. https://doi.org/10.1021/acssuschemeng.0c00443.

- (33) Cuminet, F.; Caillol, S.; Dantras, É.; Leclerc, É.; Ladmiral, V. Neighboring Group Participation and Internal Catalysis Effects on Exchangeable Covalent Bonds: Application to the Thriving Field of Vitrimer Chemistry. *Macromolecules* **2021**, *54*, 3927–3961. https://doi.org/10.1021/acs.macromol.0c02706.
- Wang, C.; Singh, A.; Rognerud, E. G.; Murray, R.; Musgrave, G. M.; Skala, M.; Murdy, P.; DesVeaux, J. S.; Nicholson, S. R.; Harris, K.; Canty, R.; Mohr, F.; Shapiro, A. J.; Barnes, D.; Beach, R.; Allen, R. D.; Beckham, G. T.; Rorrer, N. A. Synthesis, Characterization, and Recycling of Bio-Derivable Polyester Covalently Adaptable Networks for Industrial Composite Applications. *Matter* **2024**, *7*, 550–568. https://doi.org/10.1016/j.matt.2023.10.033.
- (35) Snyder, R. L.; Fortman, D. J.; Hoe, G. X. D.; Hillmyer, M. A.; Dichtel, W. R. Reprocessable Acid-Degradable Polycarbonate Vitrimers. *Macromolecules* **2018**, *51*, 389–397. https://doi.org/10.1021/acs.macromol.7b02299.
- (36) Habets, T.; Seychal, G.; Caliari, M.; Raquez, J.-M.; Sardon, H.; Grignard, B.; Detrembleur, C. Covalent Adaptable Networks through Dynamic *N,S*-Acetal Chemistry: Toward Recyclable CO<sub>2</sub>-Based Thermosets. *J. Am. Chem. Soc.* **2023**, *145*, 25450–25462. https://doi.org/10.1021/jacs.3c10080.
- (37) Ren, W.-M.; Liu, Z.-W.; Wen, Y.-Q.; Zhang, R.; Lu, X.-B. Mechanistic Aspects of the Copolymerization of CO<sub>2</sub> with Epoxides Using a Thermally Stable Single-Site Cobalt(III) Catalyst. J. Am. Chem. Soc. **2009**, 131, 11509–11518. https://doi.org/10.1021/ja9033999.
- (38) Shi, C.; Reilly, L. T.; Kumar, V. S. P.; Coile, M. W.; Nicholson, S. R.; Broadbelt, L. J.; Beckham, G. T.; Chen, E. Y.-X. Design Principles for Intrinsically Circular Polymers with Tunable Properties. *Chem* **2021**, *7*, 2896–2912. https://doi.org/10.1016/j.chempr.2021.10.004.

- (39) Capelot, M.; Unterlass, M. M.; Tournilhac, F.; Leibler, L. Catalytic Control of the Vitrimer Glass Transition. *ACS Macro Lett.* **2012**, *1* (7), 789–792. https://doi.org/10.1021/mz300239f.
- (40) Denissen, W.; Rivero, G.; Nicolaÿ, R.; Leibler, L.; Winne, J. M.; Prez, F. E. D. Vinylogous Urethane Vitrimers. *Adv. Funct. Mater.* **2015**, *25*, 2451–2457. https://doi.org/10.1002/adfm.201404553.
- (41) Hubbard, A. M.; Ren, Y.; Konkolewicz, D.; Sarvestani, A.; Picu, C. R.; Kedziora, G. S.; Roy, A.; Varshney, V.; Nepal, D. Vitrimer Transition Temperature Identification: Coupling Various Thermomechanical Methodologies. *ACS Appl. Polym. Mater.* **2021**, *3*, 1756–1766. https://doi.org/10.1021/acsapm.0c01290.
- (42) Shi, X.; Ge, Q.; Lu, H.; Yu, K. The Nonequilibrium Behaviors of Covalent Adaptable Network Polymers during the Topology Transition. *Soft Matter* **2021**, *17*, 2104–2119. https://doi.org/10.1039/D0SM01471K.
- (43) Inaba, T.; Hayashi, M. A Design of Transesterification Vitrimers with Variable Fractions of Network Defects and the Creep Characteristics. *Macromol. Chem. Phys.* **2024**, *225*, 2400037. https://doi.org/10.1002/macp.202400037.
- (44) Ricarte, R. G.; Tournilhac, F.; Leibler, L. Phase Separation and Self-Assembly in Vitrimers: Hierarchical Morphology of Molten and Semicrystalline Polyethylene/Dioxaborolane Maleimide Systems. *Macromolecules* **2018**, *52*, 432–443. https://do.org/10.1021/acs.macromol.8b02144.
- (45) Yang, Z.; Wang, Q.; Wang, T. Dual-Triggered and Thermally Reconfigurable Shape Memory Graphene-Vitrimer Composites. *ACS Appl. Mater. Interfaces* **2016**, *8*, 21691–21699. https://doi.org/10.1021/acsami.6b07403.

- (46) Chen, M.; Zhou, L.; Wu, Y.; Zhao, X.; Zhang, Y. Rapid Stress Relaxation and Moderate Temperature of Malleability Enabled by the Synergy of Disulfide Metathesis and Carboxylate Transesterification in Epoxy Vitrimers. *ACS Macro Lett.* **2019**, *8*, 255–260. https://doi.org/10.1021/acsmacrolett.9b00015.
- (47) Debnath, S.; Kaushal, S.; Ojha, U. *ACS Appl. Polym. Mater.* **2020**, *2*, 1006–1013. https://doi.org/10.1021/acsapm.0c00016
- (48) Han, J.; Liu, T.; Hao, C.; Zhang, S.; Guo, B.; Zhang, J. *Macromolecules* **2018**, *51*, 6789–6799. https://doi.org/10.1021/acs.macromol.8b01424
- (49) Singer, F. N.; Deacy, A. C.; McGuire, T. M.; Williams, C. K.; Buchard, A. Chemical Recycling of Poly(Cyclohexene Carbonate) Using a Di-Mg<sup>II</sup> Catalyst. *Angew. Chem. Int. Ed.* **2022**, *61*, e202201785. https://doi.org/10.1002/anie.202201785.
- (50) Yu, Y.; Gao, B.; Liu, Y.; Lu, X.-B. Efficient and Selective Chemical Recycling of CO <sub>2</sub> Based Alicyclic Polycarbonates via Catalytic Pyrolysis. *Angew. Chem. Int. Ed.* **2022**, *61*, e202204492. https://doi.org/10.1002/anie.202204492.
- (51) McGuire, T. M.; Deacy, A. C.; Buchard, A.; Williams, C. K. Solid-State Chemical Recycling of Polycarbonates to Epoxides and Carbon Dioxide Using a Heterodinuclear Mg(II) Co(II) Catalyst. *J. Am. Chem. Soc.* **2022**, *144*, 18444–18449. https://doi.org/10.1021/jacs.2c06937.
- (52) Rosetto, G.; Vidal, F.; McGuire, T. M.; Kerr, R. W. F.; Williams, C. K. High Molar Mass Polycarbonates as Closed-Loop Recyclable Thermoplastics. *J. Am. Chem. Soc.* **2024**, *146*, 8381–8393. https://doi.org/10.1021/jacs.3c14170.
- (53) Guerin, W.; Diallo, A. K.; Kirilov, E.; Helou, M.; Slawinski, M.; Brusson, J.-M.; Carpentier, J.-F.; Guillaume, S. M. Enantiopure Isotactic PCHC Synthesized by Ring-Opening

Polymerization of Cyclohexene Carbonate. *Macromolecules* **2014**, *47*, 4230–4235. https://doi.org/10.1021/ma5009397.

(54) Kumar, V.; Kuang, W.; Fifield, L. S. Carbon Fiber-Based Vitrimer Composites: A Path toward Current Research That Is High-Performing, Useful, and Sustainable. *Materials* **2024**, *17*, 3265. https://doi.org/10.3390/ma17133265.

# For Table of Contents Only

